Development of a Novel High Power Sub-THz Second Harmonic Gyrotron

T. Notake,[1,2,*] T. Saito,[2] Y. Tatematsu,[2] A. Fujii,[2] S. Ogasawara,[2] La Agusu,[2] I. Ogawa,[2] and T. Idehara[2]

[1]*Tera-Photonics Laboratory, RIKEN, 519-1399, Aramaki Aza Aoba, Aoba-ku, Sendai, Miyagi 980-0845, Japan*

[2]*Research Center for Development of Far-Infrared Region, University of Fukui, Fukui 910-8507, Japan*

V. N. Manuilov

Nizhny Novgorod State University, Radiophysical Faculty, Nizhny Novgorod 603600, Russia

(Received 24 May 2009; published 23 November 2009)

Record-breaking high power coherent radiation at a subterahertz frequency region from a gyrotron utilizing second harmonic resonance modes was attained with a simple cavity. In order to aim at high power and high frequency simultaneously, the oscillation mode was selected carefully enough to realize stable radiation free from mode competition. The cavity radius was determined from the viewpoints of the oscillation frequency, the coupling coefficient between the electron beam, and the rf-electric field. The cavity length was also optimized for the highest perpendicular efficiency. In addition, a new electron gun which is capable of generating a thin laminar beam for a large current was introduced. Consequently, single mode second harmonic radiation with powers of 52 and 37 kW at frequencies of about 349 and 390 GHz, respectively, was achieved.

DOI: 10.1103/PhysRevLett.103.225002 PACS numbers: 52.70.−m

The importance of the development of terahertz (THz) radiation sources has been increasing owing to their various outstanding availabilities [1–5]. Gyrotrons are unique high power radiation sources in the frequency region from GHz to THz. Research of gyrotron development has progressed toward obtaining high frequency and high power radiation. High frequency gyrotrons with frequency up to 1 THz have been demonstrated although their powers are still low [6,7]. On the other hand, high power gyrotrons with power of no less than 2 MW at frequencies lower than 170 GHz have been also developed for nuclear fusion plasma heating [8,9].

We have tried to develop a gyrotron simultaneously realizing high frequency and high power. High frequency gyrotrons require extremely high magnetic fields because gyrotrons are based on electron cyclotron maser instability. A pulse magnet system has been often used to supply such high magnetic fields. However, a gyrotron involving the pulse magnet system is not suitable for practical uses. Therefore, we have made use of second harmonic (SH) resonance to reduce difficulty on generating high magnetic fields. On the other hand, generation of high power radiations by utilizing SH resonance is more difficult than that with fundamental resonance because the risk of mode competition increases. Moreover, the perpendicular efficiency decreases as a general rule. Despite these difficulties, by developing a new powerful electron gun, carefully selecting resonant modes and, in particular, optimizing the cavity configuration, we have succeeded in generating single mode SH radiations with powers of 52 and 37 kW at frequencies of 349 and 390 GHz, respectively. These are the highest radiation power so far obtained by a SH gyrotron in the sub-THz frequency region.

High power sub-THz gyrotrons give very good perspective in many application fields such as collective Thomson scattering (CTS) diagnostics in nuclear fusion plasmas [10,11], THz communication [12], cloud radar [2], nonlinear THz spectroscopy [13].

Single mode oscillation of the design mode becomes critical for high power gyrotrons even for fundamental mode gyrotrons [8,14–16]. Single mode SH oscillation becomes more difficult because of competition with fundamental modes. An approach to suppression of mode competition was use of an iris at the output end of the straight section of the cavity and a motheye vacuum window [17]. Selective increase in the Q value of SH modes were expected. A maximum single mode power of 15 kW at 417 GHz was obtained with this method. However, complicated structure may reduce reliability. Moreover, increase in the Q value is not suitable to high power operation.

We have adopted another approach: the use of a simple cavity and thorough exploration of the best mode. Many candidate modes were selected with no restriction and isolation from neighboring fundamental and SH modes was carefully examined. Figure 1 plots the mode spectra of TEmn modes. Upper and lower lines correspond to the SH and the fundamental modes, respectively. This figure

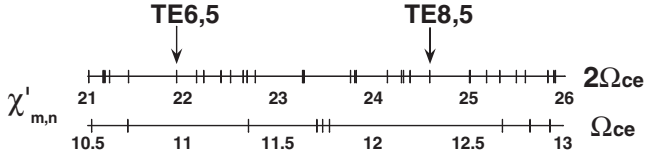

FIG. 1. Mode spectra of TE mode for second harmonic and fundamental resonance.

shows that the TE6,5 and TE8,5 modes are well isolated from neighboring modes in the dense SH mode distribution. In particular, these modes are isolated very well from fundamental modes. Therefore, both the TE6,5 and TE8,5 modes were chosen as oscillation modes.

To further improve mode separation, a cavity with a rather small radius was employed. This led to need of a thin electron beam. Then, a new electron gun which can generate a large current with high quality even in a small beam radius was developed [18,19].

Once the oscillation modes are determined, the cavity radius R_c should be optimized with a comprehensive consideration of radiation frequency and the coupling between the rf-electric field and the electron beam. The required radiation frequency of around 400 GHz was determined considering the optimum conditions for CTS diagnostics in the large helical device [11]. As for the beam-filed coupling, it is important to set the radius R_b of the electron beam entering into the cavity at the optimum value. The R_c was set to be 2.99 mm. For this radius, the resonance frequencies are 350 and 390 GHz for TE6,5 and TE8,5 modes, respectively.

The coupling coefficients defined by the following expression [20] are shown in Fig. 2 for the two modes.

$$C_{BF} = \frac{\chi'^2_{mn} J^2_{m\pm s}(\chi'_{mn} R_b/R_c)}{\pi R_c^2(\chi'^2_{mn} - m^2) J^2_m(\chi'_{mn})}. \quad (1)$$

Here, χ'_{mn} and s stand for the nth zero of derivative of the mth-order first kind Bessel function and harmonic number, respectively. The + and − signs mean counter- and corotating modes, respectively. The best coupling takes place for both modes when R_b is around 1.35 mm. According to numerical simulation of the new electron gun, however, it was found that operation with a low cathode magnetic field to compress the R_b to 1.35 mm caused turbulent beam flow. Then, the second peaks of the coupling around 1.9 mm were chosen. Even for the second peak coupling, high power radiations can be expected as long as the length of the cavity L_c is optimized. Dependences of the perpendicular efficiencies for TE6,5 and TE8,5 modes on L_c were calculated based on a nonlinear theory [21]. Figure 3 plots the results. Here, the cathode voltage V_k of 60 kV, the beam current I_b of 7 A and the pitch factor α of 1.3, which were typical parameters in the gun design, were used for the calculation. R_b was slightly shifted for the sake of the maximum coupling at the second peak for each mode. The perpendicular efficiencies are nearly maximum at 12 mm for both modes. Thus, L_c was determined to be 12 mm. The minimum starting currents of the TE6,5 and TE8,5 modes are nearly as low as those of the neighboring fundamental modes.

Based on these design consideration, a demountable gyrotron was fabricated and installed into an 8 T superconducting magnet. The gyrotron has no inner mode converter and the generated electromagnetic waves are propagated through a collector and radiated via an output vacuum window made of a single crystal sapphire with thickness of 2.5 mm. Auxiliary coils are also equipped around the electron gun for controlling R_b. Operational characteristics of the gyrotron were studied for various parameters such as the magnetic field at the cavity B_c, V_k, I_b, the anode voltage V_a and the gun coil current I_g which strongly affects R_b. Dependence of radiation intensity on B_c for $V_k = -55.8$ kV, $V_a = -40$ kV, $I_b = 11$ A, and $I_g = 150$ A is shown in Fig. 4(a). Here, each voltage was defined with respect to the grounded collector. The radiation power was guided from the vacuum window to a pyroelectric detector via an oversized waveguide. The typical pulse width was 2 μs in the experiment, and signal intensities shown in Fig. 4 were an averaged power during the pulse width detected at each B_c. Many radiations originated from various modes were observed over a wide region. To separate SH radiations from fundamental ones, a high-pass filter with a cutoff frequency of 303 GHz was inserted in front of the detector. The signals for this case are shown in Fig. 4(b). We have succeeded to obtain two distinguishing SH radiations at around of 6.87 and 7.70 T. For mode identification, starting currents for

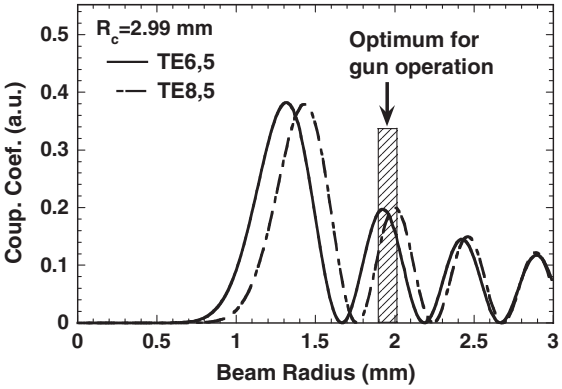

FIG. 2. Coupling coefficients for TE6,5 and TE8,5 modes as a function of beam radius. The cavity radius of 2.99 mm is adopted.

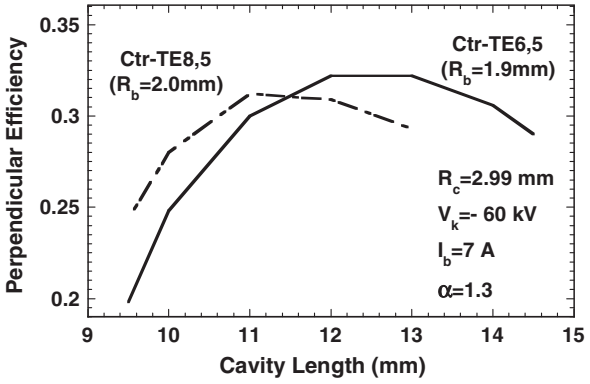

FIG. 3. Perpendicular efficiencies for TE6,5 and TE8,5 modes as a function of cavity length. The efficiencies are calculated based on the nonlinear single mode theory.

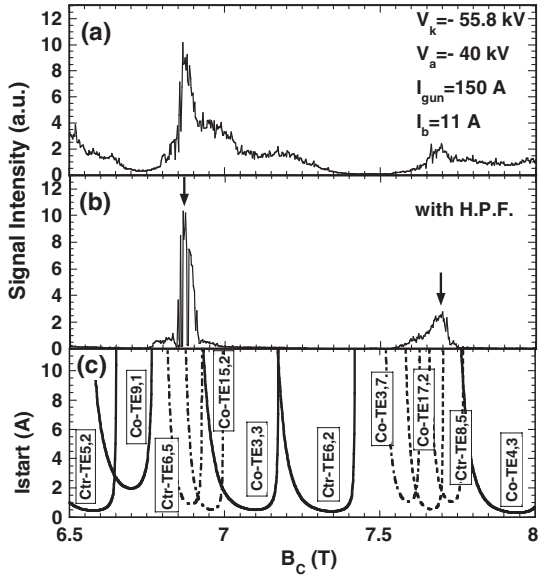

FIG. 4. Radiation characteristics (a),(b) and starting currents calculation (c) on the magnetic field B_c. In the calculation, $V_k = -55.8$ kV, $R_b = 1.85$ mm, and $\alpha = 1.3$ are assumed.

SH modes are shown with dashed lines in Fig. 4(c). Here, it should be noted that the oscillation modes which can be excited at nearby 6.87 and 7.70 T are only SH modes. Starting currents of fundamental modes also plotted with solid lines in Fig. 4(c). From comparison between experimental data and starting current calculation two peaks in Fig. 4(b) are identified as the two design modes, TE6,5 and TE8,5 modes, respectively.

Radiation frequencies of the two SH peaks were measured with a Fabry-Perot interferometer (FPI). Figure 5 shows the detected signal intensity transmitted through the interferometer as a function of the distance between reflecting meshes. The measurement was done at the $B_c = 6.87$ T which is pointed out explicitly with an arrow in Fig. 4(b). The periodic interference pattern confirms single mode oscillation of the SH mode. Irregularity in the data is due to measurement of pulse-to-pulse manner. The averaged interval between neighboring peaks is 0.430 mm. This corresponds to 349 GHz although there is an error of about 3 GHz due to variance in the data. However, the measured frequency is almost equal to the theoretical resonant frequency of TE6,5 mode, 350 GHz. In a similar way, radiation frequency at the magnetic field of 7.70 T was deduced as roughly 390 GHz. There are mainly two possibilities for this radiation, TE8,5 mode with the resonant frequency of 392 GHz, and TE17,2 mode with the resonant frequency of 389 GHz. The frequency measurement with the FPI cannot discriminate this frequency difference. However, judging from the oscillation region of the B_c, the radiation at 7.70 T must be the TE8,5 mode. The radiation observed at around 7.65 T is likely the TE17,2 mode. Therefore, single mode oscillation was successfully demonstrated for both the two design modes, TE6,5 and TE8,5 modes.

Power measurements were carried out by using a water load installed just outside of the vacuum window. Radiation power was determined from the rate of temperature rise of the water. The gyrotron was operated with the pulse width of 1 μs and the repetition rate of 10 Hz. To determine the radiation power accurately, reflections of sub-THz frequency waves off the sapphire vacuum window and the glass surface of the water load should be taken into consideration. Complex permittivities of the sapphire and the glass were directly measured by THz time domain spectroscopy method [22] and the reflection coefficients were evaluated. In the present Letter, power data corrected with the reflection coefficients are shown.

At first, to decide the optimum injection beam radius for high power radiations by the TE6,5 mode, power dependence on I_g was investigated for $V_k = -57.7$ kV and $I_b = 5$ A. The highest power was obtained with $I_g = 150$ A. This current resulted in R_b of 1.85 mm almost equal to the design beam radius. The same result was obtained for TE8,5 radiation. Then, I_g was fixed at 150 A.

The dependences of the two SH radiation powers on the beam current I_b were studied with V_k of about -57 kV. The result is shown in Fig. 6. Here, B_c were slightly

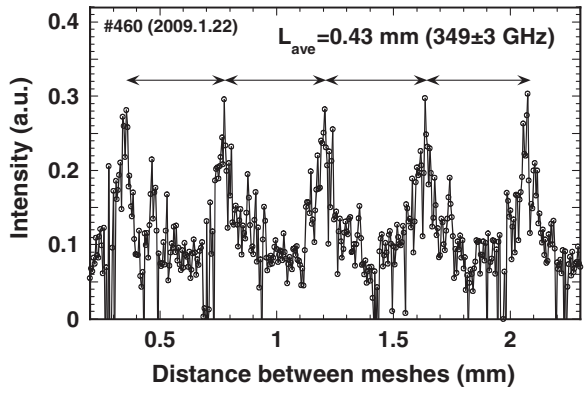

FIG. 5. Interference signals measured at the magnetic field of 6.87 T with Fabry-Perot interferometer.

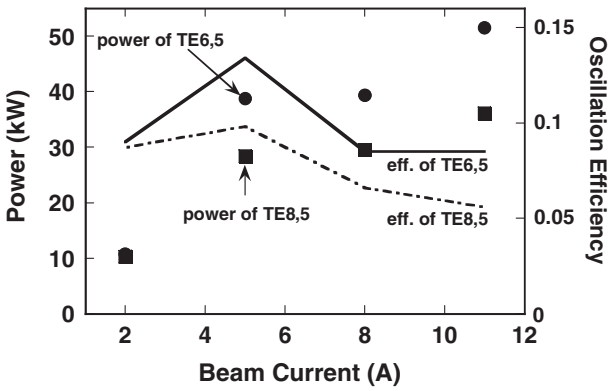

FIG. 6. Radiation powers and oscillation efficiencies of TE6,5 and TE8,5 modes as a function of beam current. Here, V_k is about -57 kV and I_g is 150 A.

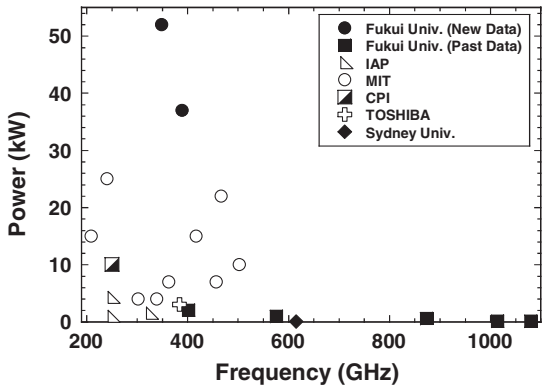

FIG. 7. Development status of second harmonic gyrotrons in the radiation power and frequency space. Data with various pulse widths are contained.

adjusted for each data points under confirmation of SH single mode oscillation with FPI. Closed circles and squares show radiation powers for the TE6,5 and the TE8,5 modes, respectively. Both powers gradually increased with I_b. The maximum radiation powers of 52 and 37 kW at frequencies of about 349 and 390 GHz for the TE6,5 and TE8,5 modes, respectively, were achieved at $I_b = 11$ A. Oscillation efficiencies are plotted by the solid and dash-dotted lines. The maximum efficiency of 14% was attained for the TE6,5 mode at 5 A. However, they decreased for I_b larger than 5 A. The oscillation efficiency is related to the perpendicular efficiency $\eta_\perp$ with the normalized perpendicular velocity β_p, the relativistic factor γ_0, diffractive quality factor Q_{diff} and Ohmic quality factor Q_{ohm}

$$P = \frac{\beta_P^2}{2(1-\gamma_0^{-1})} \cdot \frac{I_b V_k}{1 + Q_{\mathrm{dif}}/Q_{\mathrm{ohm}}} \eta_\perp. \qquad (2)$$

Observed decreases in the efficiencies are different from the numerical calculations based on the nonlinear theory. In experiment, the quality of the electron beam, which is not considered in the calculations, may degrade due to the space charge effect or some unknown effect as I_b increases. To overcome the degradation of the beam quality, higher acceleration voltage must be advisable. However, the available voltage of the power supply is limited at the moment. This problem will be resolved by establishing a new power supply system.

Figure 7 shows the state-of-the-art of development of high frequency SH gyrotron [23]. New results indicated by the closed circles have shown a large improvement of the radiation power in the sub-THz frequency region. Although the highest power so far obtained in the 400 GHz region is 22 kW at 467 GHz [17], single mode oscillation was not proved. The highest single mode oscillation power was less than 10 kW at 467 GHz and 15 kW at 417 GHz (see Table II in Ref. [17]). These powers were obtained by a complex combination of the iris cavity and the motheye window. We have demonstrated more than 50 kW single mode oscillation with a simple cavity and careful selection of oscillation modes. Moreover, 37 kW single mode oscillation at almost 400 GHz was obtained with the same cavity. This shows reliability of our approach. Then, we can extrapolate to higher power.

In summary, we have succeeded in more than 50 kW single mode oscillation of SH modes. This is based on careful mode selection and integrated consideration about the electron beam optics. The present result gives good perspective to achieve a level of 100 kW in the sub-THz frequency region. This goal may be realized with improvement of the electron gun and enhancement of the coupling between the electron beam and the rf-electric field by further optimization of the cavity configuration.

*notake@riken.jp

[1] A. V. Gaponov-Grekhov *et al.*, *Applications of High-Power Microwaves* (Artech House, Inc., Boston, 1994), ISBN 0-89006-699-x.
[2] W. M. Manheimer, Phys. Plasmas **1**, 1721 (1994).
[3] T. Tatsukawa *et al.*, Int. J. Infrared Millim. Waves **21**, 1155 (2000).
[4] H. Hoshizuki *et al.*, Int. J. Infrared Millim. Waves **26**, 1531 (2005).
[5] C. Song *et al.*, J. Am. Chem. Soc. **128**, 11385 (2006).
[6] T. Idehara *et al.*, Int. J. Infrared Millim. Waves **27**, 319 (2007).
[7] M. Yu. Glyavin *et al.*, Phys. Rev. Lett. **100**, 015101 (2008).
[8] K. Sakamoto *et al.*, Nature Phys. **3**, 411 (2007).
[9] K. Felch *et al.*, Nucl. Fusion **48**, 054008 (2008).
[10] H. Bindslev *et al.*, Phys. Rev. Lett. **97**, 205005 (2006).
[11] T. Notake *et al.*, Rev. Sci. Instrum. **79**, 10E732 (2008).
[12] Michael J. Fitch and Robert Osiander, Johns Hopkins APL Tech. Dig. **25**, 348 (2004).
[13] W. D. Moerner, *Persistent Spectral Hole-Burning* (Springer-Verlag, Berlin, 1988).
[14] Y. Carmel *et al.*, Phys. Rev. Lett. **50**, 112 (1983).
[15] K. E. Kreischer and R. J. Temkin, Phys. Rev. Lett. **59**, 547 (1987).
[16] D. R. Whaley *et al.*, Phys. Rev. Lett. **75**, 1304 (1995).
[17] S. Spira-Hakkarainen, K. E. Kreischer, and R. J. Temkin, IEEE Trans. Plasma Sci. **18**, 334 (1990).
[18] A. L. Goldenberg *et al.*, Radiophys. Quantum Electron. **48**, 741 (2005).
[19] V. N. Manuilov *et al.*, Int. J. Infrared Millim. Waves **29**, 1103 (2008).
[20] M. V. Kartikeyan, E. Borie, M. K. A. Thumm, *Gyrotrons* (Springer-Verlag, Berlin, 2004).
[21] B. G. Danly and R. J. Temkin, Phys. Fluids **29**, 561 (1986).
[22] M. Hangyo *et al.*, Meas. Sci. Techol. **13**, 1727 (2002).
[23] M. Thumm, Wissenschaftliche Berichte Report No. FZKA7392, 2008. Research report of Research Center, Karlsruhe University.